

Combined spatial- and time-division-multiplexing scheme for fiber grating sensors with drift-compensated phase-sensitive detection

Y. J. Rao, A. B. Lobo Ribeiro,* and D. A. Jackson

Applied Optics Group, Physics Laboratory, University of Kent, Canterbury, Kent CT2 7NR, UK

L. Zhang and I. Bennion

Photonics Research Centre, Department of Electronic Engineering, Aston University, Birmingham B4 7ET, UK

Received July 5, 1995

A combined spatial- and time-division-multiplexing topology with drift-compensated high-resolution wavelength-shift detection is reported for fiber Bragg grating sensors. An eight-element grating sensor array is demonstrated based on this topology. A resolution of $\sim 1.2 \mu\epsilon$ over a range of $\sim 1.5 m\epsilon$ with a measurement bandwidth of 30 Hz ($\sim 0.22 \mu\epsilon/\sqrt{\text{Hz}}$) has been achieved for quasi-static strain measurement. © 1995 Optical Society of America

Fiber Bragg grating (FBG) sensors represent one of the most exciting developments in the field of optical fiber sensors in recent years and are currently the subject of intensive research. They have a number of advantages over other implementations of fiber-optic sensors. One of the main features is that they can be multiplexed in a manner similar to that used for fiber-optic sensors, such as wavelength-division multiplexing, time-division multiplexing (TDM), and their combinations,¹⁻⁴ making quasi-distributed sensing feasible in practice. However, for many practical applications in which FBG sensors must be located randomly in a network for multipoint measurements, interchangeability and ease of replacement in the event of damage without recalibration will be a critical issue. For such applications it is not feasible to employ series multiplexing topologies, such as wavelength-division and TDM, which are based on a single fiber link arrangement. To overcome problems associated with series multiplexing topologies, we recently demonstrated a parallel topology based on spatial-division multiplexing (SDM).⁵ In this Letter we report a modification of this topology that combines both SDM and TDM. An eight-element FBG sensor system based on this (SDM + TDM) topology is demonstrated for quasi-static strain measurement. A drift-compensated phase-sensitive detection scheme is used to eliminate the thermal drift of the wavelength scanner, which employs a local reference FBG held at constant strain and temperature in conjunction with the sensing FBG.⁶

A schematic diagram of this (SDM + TDM) system is shown in Fig. 1. A pigtailed temperature-stabilized superluminescent diode (SLD) with a bandwidth of $\sim 18.5 \text{ nm}$ (818–836.5 nm), supplied by Superlum Ltd. (Moscow, Russia), was used as the light source. The output optical power from the single-mode fiber was greater than 1.5 mW. The 1×8 fiber-optic splitter shown in Fig. 2 was specially designed for this system. There are four output ports, with each port containing two fiber transmission lines with differ-

tial delay lengths of 40 m, corresponding to a time delay of 400 ns. FBG sensors were connected to the ends of these fiber lines by fiber connectors (FC's). Eight FBG's were deployed in this network, as indicated in Fig. 1. It would be feasible to interrogate another eight FBG's by duplicating part of the network without reduction in the signal-to-noise ratio of each sensor, as also indicated in Fig. 1. The source was pulsed at a frequency of $\sim 1.1 \text{ MHz}$ with a pulse width of $\sim 300 \text{ ns}$ (duty cycle $\sim 1/3$). The pulsed light was launched into the wavelength scanner (WS) and the 1×8 splitter. The return pulse signals from the FBG sensors were coupled back into the splitter and detected by an array of four avalanche photodetectors (APD) followed by integral separated high-speed amplifiers (10 MHz). The signals from the APD array were selected by a switch (SW1). Thus each APD receives the returned signals from two FBG's separated in time by $\sim 400 \text{ ns}$. These two signals were separated by two

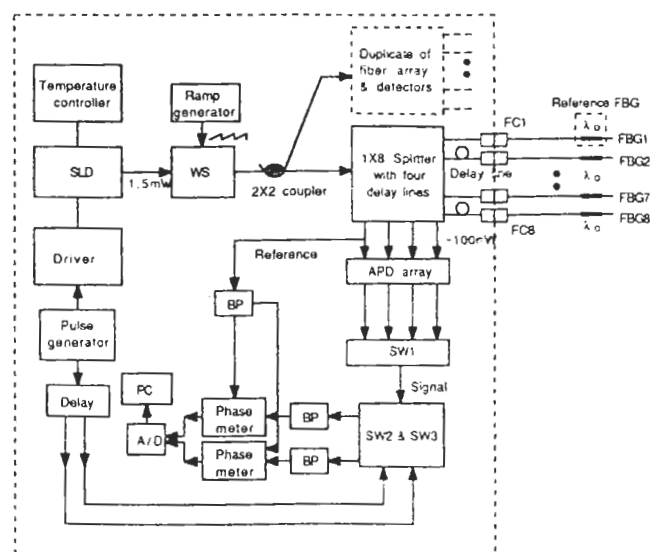


Fig. 1. Schematic diagram of the multiplexing system.

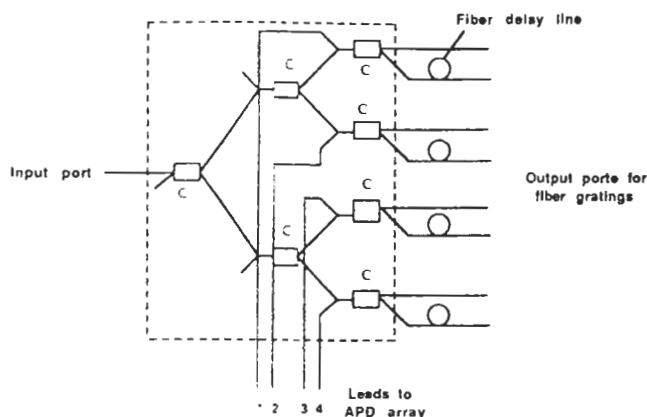


Fig. 2. Diagram of the specially designed 1×8 fiber splitter.

high-speed switches (SW2 and SW3) controlled by the delayed electric pulses produced by the pulse generator as shown in Fig. 1.

The phase information contained in the interference signal was recovered by the pseudoheterodyne technique.⁷ The WS used in this research was a bulk Michelson interferometer developed by Queensgate Instruments Ltd. The piezoelectric transducer in the WS was driven by a ramp (serrrodyne) modulation function at a frequency of 300 Hz. As the optical path difference (OPD) in the WS determines the free spectral range or the total absolute measurement range, it is necessary to determine the OPD of the WS precisely. In this study we achieve this by using the white-light interferometric scheme.⁵ A fiber-based Fabry-Perot cavity, formed by the cleaved end of the fiber and a mirror mounted on a translation stage, was incorporated into the network. The gap between the cleaved fiber end and the mirror was initially set with the fiber end touching the mirror (i.e., zero OPD). When the length of the Fabry-Perot cavity is tuned to be equal to that of the WS, the maximum amplitude of the interference signal is observed. The displacement between the fiber end and the mirror is then equal to the cavity length of the WS. The OPD of the WS used here was found to be ~ 0.7 mm (equal to a free spectral range of ~ 0.98 nm). After band-pass filtering (BP's) at the fundamental frequency of the serrrodyne signal, the sinusoidal output corresponding to each sensing FBG was sent to a phase meter so that we could determine the phase change relative to the reference FBG (here the reference FBG is FBG1). The output phase signal from the phasemeter was sent to a personal computer (PC) via a 12-bit analog-to-digital converter (A/D). The resolution of the phasemeter was 0.1 deg, corresponding to a wavelength resolution of $\sim 0.27 \times 10^{-3}$ nm for the free spectral range of the WS (0.98 nm). The sensing and reference FBG's used here were made from a standard 800-nm single-mode fiber that was sensitized by soaking in a high-pressure hydrogen atmosphere. The nominal Bragg wavelength and reflectivity of the FBG's were all ~ 830 nm and $\sim 90\%$, respectively, with a bandwidth of ~ 0.2 nm. The reference FBG was deployed strain free and located in the same temperature environment as the sensing FBG's.

The detected signals from this eight-element FBG array are shown in Fig. 3(a). To show the delayed pulses clearly, we adjusted the amplitudes of these pulses by changing the joint loss within the FC's. The demultiplexed signals corresponding to four FBG sensors are shown in Fig. 3(b). Cross talk between two adjacent TDM channels was measured to be < -36 dB.

To obtain the strain-to-phase shift responsivity, we mounted the sensing FBG between a fixed block and a precision translation stage, separated by a distance of ~ 40 cm. The experimental results of the static-strain measurement are shown in Fig. 4(a). The measured strain-to-phase shift responsivity was ~ 237 deg/m ϵ , corresponding to a strain-to-wavelength coefficient of $\sim 0.64 \times 10^{-3}$ nm/ $\mu\epsilon$. For the thermal drift-compensated measurement, we introduced a quasi-static strain by applying a known displacement of the sensing FBG, using a cylindrical piezoelectric transducer (for this case, one of the FBG ends was mounted on the cylindrical piezoelectric transducer rather than on the translation stage). The experimental results of the quasi-strain measurement are shown in Fig. 4(b). We applied several ~ 0.2 -Hz strain steps of $\sim 9 \mu\epsilon$ peak-to-peak amplitude to the sensing FBG. It can be seen that a strain resolution of $\sim 1.2 \mu\epsilon$, determined by the noise level, was achieved with a 30-Hz measurement bandwidth. The overall strain range shown in Fig. 4(a) was ~ 1.5 m ϵ ; hence the achieved range-to-resolution ratio was 1250:1. In addition, we demonstrated the interchangeability

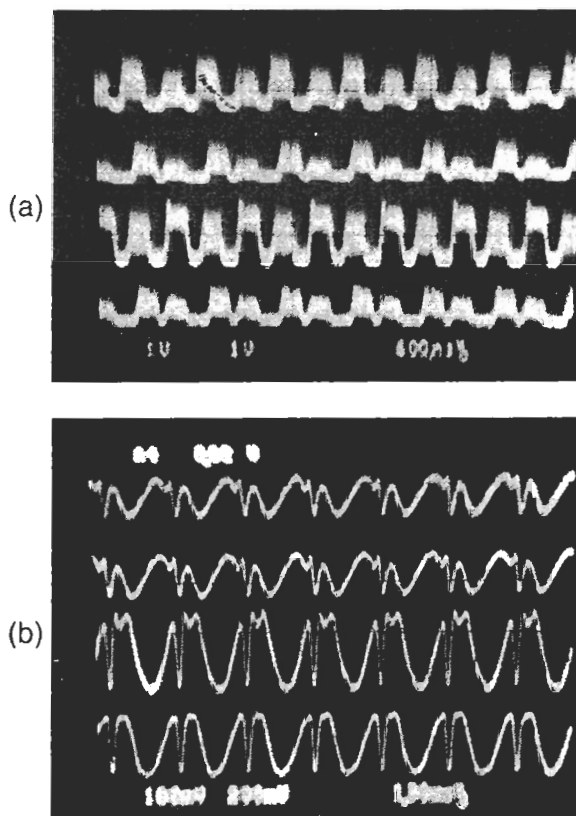


Fig. 3. Experimental waveforms. (a) Photodetected return pulse signals for eight gratings; each trace corresponds to the signals from two gratings with TDM. (b) Demultiplexed signals from four gratings.

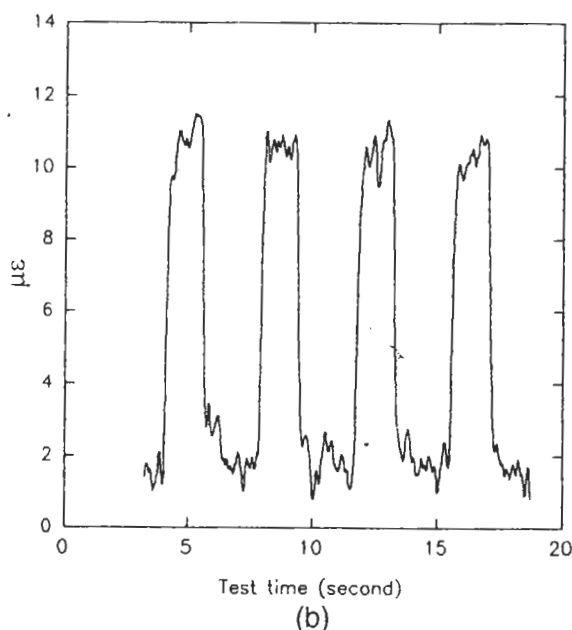
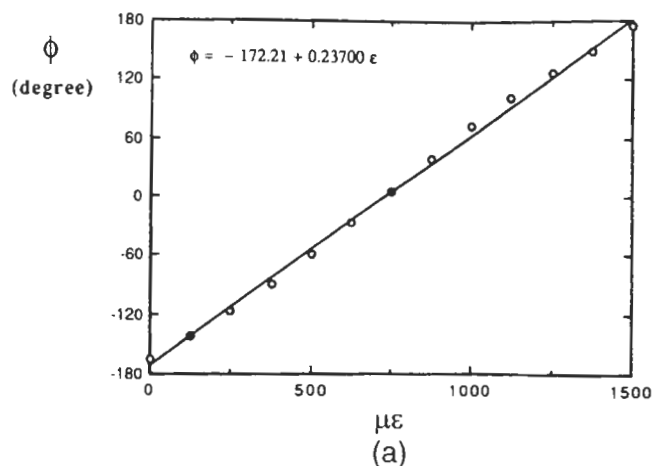


Fig. 4. Experimental results of the strain measurement: (a) static-strain measurement (ϕ is the phase change), (b) quasi-static-strain perturbation.

of this system by moving FBG sensors between the different output ports. Virtually no change in sensor performance occurred during this procedure.

In summary, we have demonstrated a combined spatial- and time-division-multiplexing topology with drift-compensated high-resolution wavelength-shift

detection for a fiber Bragg grating sensor system. An eight-element grating sensor array based on this topology is demonstrated. In principle, the network can be extended to support 16 FBG sensors without affecting the signal-to-noise ratio of each sensor. A range-to-resolution ratio of 1250:1 for quasi-static strain measurement has been achieved with a measurement bandwidth of 30 Hz ($\sim 0.22 \mu\epsilon/\sqrt{\text{Hz}}$). This parallel multiplexing topology has the following advantages when compared with series multiplexing topologies: (1) the operation wavelength ranges of the sensors can be identical and are unaffected by the number of sensors to be multiplexed, which minimizes the cost of fabricating the FBG's; (2) there is flexibility in deployment, as there is one FBG per fiber; (3) sensor interchange and replacement in the event of damage are easily accomplished (note that the wavelength of the replacement FBG does not need to be specified, and the only requirement is that its nominal wavelength must be within the bandwidth of the source). These features make this network practical and universal for many applications.

This study was partially supported by the Wellcome Trust Foundation and the Engineering and Physical Sciences Research Council. A. B. Lobo Ribeiro acknowledges the financial support of the Programa PRAXIS XXI.

*Present address, Grupo de Optoelectrónica, INESC, R. José Falcão 110, 4000 Porto, Portugal.

References

1. D. A. Jackson, A. B. Lobo Ribeiro, L. Reekie, and J. L. Archambault, *Opt. Lett.* **18**, 1192 (1993).
2. A. D. Kersey, T. A. Berkoff, and W. W. Morey, *Opt. Lett.* **18**, 1370 (1993).
3. R. S. Weis, A. D. Kersey, and T. A. Berkoff, *IEEE Photon. Technol. Lett.* **6**, 1469 (1994).
4. A. D. Kersey, *Proc. Soc. Photo-Opt. Instrum. Eng.* **2071**, 30 (1994).
5. Y. J. Rao, K. Kalli, G. P. Brady, D. J. Webb, and D. A. Jackson, *Electron. Lett.* **31**, 1009 (1995).
6. A. D. Kersey, T. A. Berkoff, and W. W. Morey, *Opt. Lett.* **18**, 72 (1993).
7. D. A. Jackson, A. D. Kersey, and M. Corke, *Electron. Lett.* **18**, 1081 (1982).
8. Y. J. Rao, D. A. Jackson, R. Jones, and C. Shannon, *J. Lightwave Technol.* **12**, 1685 (1994).